LAWRENCE
LIVERMORE
NATIONAL
LABORATORY

LLNL-JRNL-560416

TiC: Splittings, Satellites and Fine Structure in the Soft X-ray Spectroscopy of the Actinides

J. G. Tobin, S. W. Yu, B. W. Chung

June 8, 2012

Topics in Catalysis

Disclaimer

Splittings, Satellites and Fine Structure in the Soft X-ray Spectroscopy of the Actinides*

J. G. Tobin#, S.-W. Yu, and B.W. Chung
Lawrence Livermore National Laboratory, Livermore, CA, USA

*This article is based on material to be presented at the 244th National Meeting of the American Chemical Society, Philadelphia, PA, USA, August 19-23, 2012
#Corresponding Author, Tobin1@LLNL.Gov

Abstract

Perhaps the most demanding and powerful actinide spectroscopy is that using soft x-ray and VUV photons. Because of the relatively low energy and fairly small sampling depths of these photons and the corresponding electrons, it is necessary to use un-encapsulated samples with highly cleaned and well-prepared surfaces. This causes a myriad of sample containment problems for these radioactive materials. Despite these hindrances and difficulties, the soft-x-ray and ultra-violet spectroscopy of the actinides can provide an amazing level of detailed information, particularly having to do with 5f electronic structure. In this paper, the splittings, satellites and fine structure of the following actinide soft x-ray spectroscopies will be discussed: X-ray Photoelectron Spectroscopy (XPS); X-ray Absorption Spectroscopy (XAS); and Inverse Photoelectron Spectroscopy (IPES), including Bremstrahlung Isochromat Spectroscopy (BIS) and Resonant Inverse Photoelectron Spectroscopy (RIPES).

Splittings, Satellites and Fine Structure in the Soft X-ray Spectroscopy of the Actinides*

I Introduction

Despite the limitations imposed by their sometimes high levels of radioactivity, there has recently been remarkable progress in the soft X-ray spectroscopy of the actinides, particularly that of Plutonium (Pu) and Uranium (U). For example, synchrotron-radiation-based X-ray absorption spectroscopy (XAS) and X-ray photoelectron spectroscopy (XPS) played important roles in the progress of our understanding of Pu electronic structure. [1-5] This leaves only the last issues of electron correlation, including magnetic cancellation [6] and the differentiation of 5f and 6d contributions (discussed below), before a complete understanding is achieved. Two examples of the manifestations of the large spin-orbit splitting in the 5f states can be seen in Figure 1 below: the large disparity in the relative $4d_{3/2}$ intensities of Pu and U, and the presence of the pre-peak structure in U and its absence in Pu. We will return to a more thorough discussion of these features below, including a brief history of some of the splittings, satellites and fine structure in materials such as the important nuclear fuel system UO_2, [7] which also exhibits strong electron correlation. [8] Our new measurements on UO_2, using Resonant Inverse Photoelectron Spectroscopy (RIPES) and X-ray Emission Spectroscopy [9,10], indicate new satellite structure, complementing that already observed in XPS [7, 11-15], XAS [8,16] and IPES/BIS [13,17,18]. It will also be described how RIPES opens the door to the isolation of 5f and 6d contributions to the low lying unoccupied states, without the necessity of utilizing synchrotron radiation.

II Experimental

The XPS, XES and RIPES experiments upon UO_2 were carried out at Lawrence Livermore National Laboratory (LLNL), as described elsewhere [19]. A schematic of the spectrometer is shown in Figure 2. The experimental setup at LLNL for actinides research at LLNL includes a capability for Photoelectron Spectroscopy, utilizing electron detection with spin and without spin (multichannel) sensitivity, using a Phoibos 150 with a Mott detector from Specs. Fano Spectroscopy can be performed with the chirally configured He UPS sources, [6] as well as traditional XPS with the X-ray tube at AlKα and MgKα energies. The BIS, RIPES and XES were performed using an XES 350 monochromator and multichannel detector from VG Scienta. Both XPS and BIS/RIPES rely upon a mono-energetic excitation and an energy analysis of the emitted particle. The XAS and synchrotron radiation based photoelectron spectroscopy measurements were made at the Advance Light Source (ALS) at the Lawrence Berkeley National Laboratory (LBNL) [1-5, 8] and the Stanford Synchrotron Radiation Laboratory. [5]

Some of the relevant spectroscopic processes are shown in Figure 3. XPS and XES can sample the occupied density of states (ODOS) or Valence Bands (VB). IPES,BIS, RIPES and XAS sample the unoccupied density of states (UDOS) or Conduction Bands (CB). In all of these processes of photon absorption and emission, there is great selectivity derived from the electric dipole transitions with $\Delta l = +/- 1$. We will return to these issues below.

Splittings, Satellites and Fine Structure in the Soft X-ray Spectroscopy of the Actinides*

III Spectral Results and Discussion

IIIa X-ray Photoelectron Spectroscopy

As shown in Figures 3 and 4, photoelectron spectroscopy is a photon in – electron out process. Energy conservation in the process can be described as follows in equation 1.

$$h\nu = KE + B^F + \Phi \qquad \text{Eq 1}$$

Here, hv is the photon energy, KE is the kinetic energy of the electron, B^F is the binding energy of the electron relative to the Fermi Level and Φ is the work function. In our laboratory experiments, we can choose from four energies of excitation: XPS with the AlKα (hv = 1487 eV); XPS with the MgKα (hv = 1253 eV); Ultraviolet Photoelectron Spectroscopy (UPS) with HeII (hv = 40.8 eV); and UPS with HeI (hv = 21.22 eV).

There is substantial evidence of satellite structure in the photoelectron spectroscopy of the actinides, particularly for Uranium Dioxide. Two examples are shown in Figure 5: the shoulders that appear on the high binding energy sides of the U4d peaks and the 6eV and 12 eV satellites of the U4f peaks. [7] Interestingly, the satellites in the U4d and U4f features of UO_2 are not present in the U4d and U4f features of U. These satellites are not new, having been reported by Allen, Trickle and Tucker [12], Baer and Schoenes [13], and McLean, Comenares, Smith and Somorjai [14] in the early 1980s. Allen, Trickle and Tucker also reported satellites in other spectral features, such as the 5d and 5p of UO_2. [12] In our studies, we've used the XPS and its satellites in a crude way, to get sample purity & a beginning on stoichiometry, including sample degradation with time, as illustrated in Figure 5. In

our case, the satellite structure agrees with UO_2, but not U, providing evidence in support of our contention of one, not multiple U sites. Idriss and coworkers have elevated this approach to an art-form, to address detailed issues of stoichiometry. [15]

IIIb X-ray Absorption Spectroscopy

The fundamentals of the X-ray absorption spectroscopy (XAS) process are shown in Figures 3 and 6. It is necessary to have a tunable x-ray source, hence the need for synchrotron radiation. Because most of the samples of interest to us are too thick for transmission measurements, the effects of the absorption must be measured by monitoring other quantities, such as the Total Fluorescence Yield (TFY) or the Total Electron Yield (TEY). [8] In general, TFY is less-surface-sensitive than TEY.

As illustrated in Figure 1, XAS can provide great insight into the 5f electronic structure of actinides. Our work on Pu and U is built upon the pioneering work of Kalkowski, Kaindl, Brewer, and Krone upon various U compounds. [16] They reported the observation of many significant pre-peaks and satellites. One interesting result is that the pre-peak that is shown in the U5d spectrum of UO_2 in Figure 1 appears in a wide array of U materials, including U metal, UNi_5, UCu_5, UF_4, UO_2 and UO_3. Thus, the pre-peak is resilient, apparently almost independent of the chemical state of the U.

We've used the presence or absence of the prepeak to help determine the number of 5f electrons in Pu. Pre-peaks have been seen before in other systems and are well understood. The pre-edge structure in the Rare Earth 4d-4f transitions was explained in the 1970s by Dehmer, Starace, Fano, Sugar and Cooper. [20]. An

example of the pre-peak structure in the Ce4d spectra can be seen in Figure 7. [21,22] After photon absorption, the partially occupied, shallow d core level couples with the partially occupied f states, and coulombic repulsion splits the overall states with different angular momentum couplings. However, near the end of a series or with the filling of an electronic substructure, the behavior changes. The end of the series behavior was explained by Johansson et al. [23] If the excited electron fills the low lying unoccupied f states, the angular momentum coupling between the d and f states is lost and the pre-peak disappears. This is what happens with Pu: initially $(5f_{5/2})^5$, it becomes $(5f_{5/2})^6$ in the excited state and the pre-peak disappears. Thus, the loss of the prepeak in Pu means that $n \geq 5$, with one hole in the $5f_{5/2}$ manifold. For more discussion of this issue, please see Reference 5.

Another aspect of the $(5f_{5/2})^5$ structure in Pu can be seen in the 4d XAS results shown in Figure 1. The relative diminishment of the $4d_{3/2}$ in Pu is driven by the combination of a large spin-orbit splitting in the f states and dipole selection rules. This is graphically shown in Figure 8. Here, the $d_{3/2}$ to $f_{7/2}$ transitions are forbidden. For U, we expect a $(5f_{5/2})^3$ configuration and for Pu a $(5f_{5/2})^5$ configuration. As the $(5f_{5/2})$ level fills up, the $4d_{3/2}$ intensity will drop. Thus, the small $4d_{3/2}$ intensity in Pu again confirms our picture of Pu with a fairly large spin-orbit splitting in the 5f states and an occupation of 5, i.e. $(5f_{5/2})^5$.

It is useful to consider the 4d XAS in more detail. It is of interest that the U 4d XAS is nicely statistical, with relative intensities of approximately 6:4. (Figure 1) Again, this appears to be independent of chemical state: Kalkowski, Kaindl, Brewer, and Krone reported in the 1980s that the U4d XAS of U metal and UF_4 were

essentially identical. [16] It is also productive to consider a small spin-orbit splitting case, such as Ce. [21,22] The Ce 3d XAS in the lower part of Figure 7 clearly show a robust $3d_{3/2,}$ with no signs of diminishment. This is consistent with the small-spin-orbit limiting case, shown on the left side of Figure 8. Here, the overlap and intermixing of the 7/2 and 5/2 lobes is sufficient to help reduce any possibility of seeing of the effect. While Ce [22] is often touted as a surrogate for Pu, with multiple phases and a lattice expansion that parallels that in Pu [1-5], it is clear that spectroscopically they are significantly different. This data also illustrates another important point: the lifetime broadening in the XAS of Actinides can cause a loss of fine structure relative to the Rare Earths. Clearly, the Pu and U 4d XAS peaks are substantially broadened relative to the Ce 3d XAS, eliminating any chance of seeing the kind of fine structure that is observed in the Ce 3d XAS. However, despite the loss of fine structure, the relative intensities of the $4d_{5/2}$ and $4d_{3/2}$ peaks can be used to confirm that n = 5 in Pu. Below, another case will be discussed, where the 4d XAS is applied in a productive manner, despite its lifetime broadening.

The results of a recent XAS study of UO_2 are shown in Figure 9. By means of a careful calibration of the monochromator gratings and cross-calibration of the energies associated with the different levels, it was possible to put all of the XAS spectra on one energy scale and determine the distribution of the U5f, U6d and O2p in the Unoccupied Density of States (UDOS). [8,24] This is an important result, where the U5f and U6d states have been experimentally differentiated. While the occupied densities of states (ODOS) of the actinides have been studied extensively with variants of photoelectron spectroscopy, the corresponding unoccupied states have

not been studied nearly as much. This probably reflects the increased difficulty for the study of the UDOS, because of the radioactive actinides are less welcome at soft X-ray sources such as synchrotron radiation facilities (e.g. XAS) and the reduced counting rates of inverse techniques (IPES,BIS and RIPES). Despite these limitations, these experiments can be powerfully productive, as seen in Figure 9 and will be shown in the discussion of the inverse techniques next.

IIIc Inverse Photoelectron Spectroscopy and Related Techniques

Conceptually, Inverse Photoelectron Spectroscopy is very simple: run the Photoelectron Spectrosocopy process backwards, as shown in Figures 3 and 10. An incoming electron strikes a sample, causing the emission of a photon. Similar to equation 1, an energy relation governs the IPES process, as shown in Equation 2.

$$h\nu + H^F = KE + \Phi \qquad \text{Eq 2}$$

Here, hv is the photon energy, KE is the kinetic energy of the electron, H^F is the energy of the hole relative to the Fermi Level and Φ is the work function. [9,25,and 26] Of course, it is not nearly that simple. For example, it has been found that IPES has greatly reduced counting rates relative to PES, due to the reduction in the final density of states. [9,10,25, and 26] Discussion of these important details can be found elsewhere. [26]

While the term Inverse Photoelectron Spectroscopy (IPES) is broad, encompassing the whole field and its many variants, it is often used to denote only the low energy measurements [18], such as those with Geiger-Mueller tubes as detectors [25] and low energy monochromators. [26] At higher energies, the monoenergetic variant is usually called Bremstrahlung Isochromat Spectroscopy

(BIS) [13,17] and a tunable version is known as Resonant IPES or RIPES [27,28], going through core levels analogously to Resonant PES. [29] In IPES, BIS and RIPES, there is a wavelength selection in the photon detection and a mono-energetic beam of electrons is used as the excitation. (Figures 2 and 10) In this experimental setup, it is also possible to perform X-ray Emission Spectroscopy (XES), with a electron in & photon out, but the energetics and the information provided are different. We will return to XES again below.

XES $KE > B^F$ (core) Eq 3

XES $h\nu \approx B^F$ Eq 4

Baer and coworkers lead the way in the application of BIS to actinides. [13,17] Consider the data shown in Figure 11. The top panel shows a BIS spectrum for U, reported by Baer and Lang [17] in 1980. Clearly, this is beautiful work. With the advantages of 30 years hindsight, we have reinterpreted their result with a picture for U that includes a large spin-orbit splitting (on the scale of an eV) in the U5f states [4,21,30], as illustrated in the lower panel. In red is the DOS calculation by A.L. Kutepov [4,21]; In black is the DOS calculation times the inverse Fermi function, with some instrumental broadening. [30] The observation of this type of double lobed structure is powerful evidence in support of the large spin-orbit picture utilized in the analysis of Pu and U (Figure 1) and illustrated in Figure 8.

Baer and coworkers did not limit themselves to U metal: they also performed similar BIS studies near 1487 eV on the important nuclear fuel material, Uranium Dioxide. [13] About the same time, Chauvet and Baptist [18] were also investigating UO_2, using lower energy IPES (photon energies of 20.6, 25.3, 31 and 49.6 eV),

finding strong agreement with the BIS results of Baer and Schoenes. Shown in Figure 12 is our BIS spectrum for UO_2, using 915 eV excitation. Not surprisingly, our results confirm the observations of both Baer/Schoenes and Chauvet/Baptist, with a large feature a few volts above the Conduction Band Minimum (CBM). While Baer/Schoenes observed only the larger peak near 4 eV, Chauvet /Baptist reported two peaks, the larger near 4 eV and a smaller one near 10 eV, particularly at the lowest detection energies. Based upon our XAS results shown in Figure 9, our re-interpretation is that the large peak near 4 eV is the U5f and the small one near 10 eV is the U6d. [8,10] This interpretation is further supported by a consideration of the IPES cross sections. The BIS spectrum will be dominated by the 5f contribution, because the 5f cross section is about 10 times the 6d cross section at higher photon energies. However, at the lowest photon energies, the two cross sections should become comparable. [8,31]

Finally, it is useful to close our discussion with a description of a new satellite in UO_2, one that is seen in RIPES and XES and can be used to isolate the 5f from 6d components in the UDOS without resorting to the use of synchrotron radiation. As shown in Figure 13, the new results for RIPES in UO_2 [10] include dispersion with hv and a resonance and a satellite, which are separated by 14 eV. The resonance and satellite are mirrored by peaks in the XES. The resonance is weaker than that observed in Cerium Oxide [9] but much stronger than anything observed for metallic U [28].

The RIPES main and satellite peaks are due to the U5f and U6f components of the UDOS. The reasoning is as follows. (1) In BIS or IPES, the U5f cross sections

dominate the U6d cross sections. (2) However, in RIPES, a second channel opens up, which is not limited by electric dipole selection rules. The matrix element is coulombic in nature. (3) Thus, RIPES can probe the U6d states, while regular BIS does not. (4) The separation of the spectral features is twice the separation of the UDOS, i.e. Δ, because two electrons are involved. $\Delta \approx 7$ eV and $2\Delta \approx 14$ eV. (5) Hence, RIPES & XES can separate the U5f and U6d contributions to the Unoccupied Density of States (UDOS), without the utilization of synchrotron radiation. This opens the door to measurements upon more highly radioactive samples, which would be problematic, if not forbidden, at the synchrotron radiation sources. Thus, Pu is possible!

IV Conclusions

It has been shown how soft X-ray spectroscopy can provide an immense amount of important information about the electronic structure of the actinides. The subjects of discussion included: X-ray photoelectron spectroscopy (XPS), Soft x-ray absorption spectroscopy (XAS), Soft x-ray emission spectroscopy (XES), Inverse photoelectron spectroscopy (IPES), Bremstrahlung Isochromat Spectroscopy (BIS), Low energy IPES, and Resonant inverse photoelectron spectroscopy (RIPES). Our ultimate goal remains Pu and its electron correlation, including magnetization cancellation and 5f/6d differentiation.

Acknowledgements
Lawrence Livermore National Laboratory is operated by Lawrence Livermore National Security, LLC, for the U.S. Department of Energy, National Nuclear Security Administration under Contract DE-AC52-07NA27344. This work was supported by the DOE Office of Science, Office of Basic Energy Science, Division of Materials Science and Engineering.

References

Splittings, Satellites and Fine Structure in the Soft X-ray Spectroscopy of the Actinides*

1. J.G. Tobin, B.W. Chung, R. K. Schulze, J. Terry, J. D. Farr, D. K. Shuh, K. Heinzelman, E. Rotenberg, G.D. Waddill, and G. Van der Laan, , Phys. Rev. B **68**, 155109 (2003).
2. K.T. Moore, M.A. Wall, A.J. Schwartz, B.W. Chung, D.K. Shuh, R.K. Schulze, and J.G. Tobin, Phys. Rev. Lett. **90**, 196404 (2003).
3. G. van der Laan, K.T. Moore, J.G. Tobin, B.W. Chung, M.A. Wall, and A.J. Schwartz, Phys. Rev. Lett. **93**, 097401 (2004).
4. J.G. Tobin, K.T. Moore, B.W. Chung, M.A. Wall, A.J. Schwartz, G. van der Laan, and A.L. Kutepov, Phys. Rev. B **72**, 085109 (2005).
5. J.G. Tobin, P. Söderlind, A. Landa, K.T. Moore, A.J. Schwartz, B.W. Chung, M.A. Wall, J.M. Wills, R.G. Haire, and A.L. Kutepov, J. Phys. Cond. Matter **20**, 125204 (2008).
6. S.W. Yu, J.G. Tobin, and P. Söderlind**,** J. Phys. Cond. Matter **20**, 422202 (2008), Fast Track Communication.
7. J.G. Tobin, S.-W. Yu, B.W. Chung, G.D. Waddill and J.D. Denlinger, J. Vac. Sci. Tech. **A 29,** 031504 (2011).
8. S.-W. Yu, J. C. Crowhurst, J. G. Tobin, S. Sharma, J. K. Dewhurst, P. Olalde-Velasco, W. L. Yang, and W. J. Siekhaus, Phys. Rev. B **83**, 165102 (2011).
9. J.G. Tobin, S.W. Yu, B.W. Chung, G.D. Waddill, E. Damian, L. Duda and J. Nordgren, Phys. Rev B **83**, 085104 (2011).
10. J.G. Tobin and S.-W. Yu, Phys. Rev. Lett, **107,** 167406 (2011).
11. B.W. Veal and D. J. Lam, Phys. Rev. B 10, 4902 (1974); Phys. Lett.A 49, 466 (1974).
12. G.C. Allen, I.R. Trickle and P.M. Tucker, Philos. Mag. B **43**, 689 (1981).
13. Y. Baer and J. Schoenes, Solid State Commun. **33**, 885 (1980).
14. W. McLean, C.A. Colmenares, R.L. Smith and G.A. Somorjai, Phys. Rev. B **25**, 8 (1982).
15. H. Idriss, Surface Science Reports **65**, 67 (2010).
16. G. Kalkowski, G. K. Kaindl, W. D. Brewer, and W. Krone, Phys. Rev. B **35**, 2667

(1987).

17. Y. Baer and J.K. Lang, Phys. Rev. B **21**, 2060 (1980).
18. G. Chauvet and R. Baptist, Solid State Commun. 43, 793 (1982).
19. S.-W. Yu, J. G. Tobin, and B. W. Chung**,** Rev. Sci. Instruments **82**, 093903 (2011).
20. J.L. Dehmer, A.F. Starace, U. Fano, J. Sugar, and J.W. Cooper, Phys. Rev. Lett. **26**, 1521 (1971).
21. J.G. Tobin, S.-W. Yu, B.W. Chung, G.D. Waddill and AL Kutepov, IOP Conf. Series: Materials Science and Engineering **9** (2010).
22. K.T. Moore, B.W. Chung, S.A. Morton, S. Lazar, F.D. Tichelaar, H.W. Zandbergen, P. Söderlind, G. van der Laan, A.J. Schwartz, and J.G. Tobin, Phys. Rev. B **69**, 193104 (2004).
23. L. I. Johansson, J. W. Allen, I. Lindau, M. H. Hecht, and S. B. M. Hagström, Phys. Rev. B **21**, 1408 (1980).
24. S.-W. Yu, J. G. Tobin, P. Olalde-Velasco, W. L. Yang, and W. J. Siekhaus, J. Vac. Sci. Tech. A. **30**, 011402 (2012).
25. B. Knapp and J. Tobin, Phys. Rev. B **37**, 8656 (1988).
26. J.G. Tobin, "Photoemission and Inverse Photoemission," in "Determination of Optical Properties," Vol. VIII in Physical Methods of Chemistry, 2nd edition, Ed. B.W. Rossiter and R.C. Bretzold, John Wiley and Sons, New York, 1993, and references therein.
27. P. Weibel, M. Grioni, D. Malterre, B. Dardel, and Y. Baer, Phys. Rev. Lett. 72, 1252 (1994).
28. M. Grioni et al., J. Electron Spectrosc. Relat. Phenom. 101–103, 713 (1999).
29. S.R. Mishra, T.R. Cummins, G. D. Waddill, W.J. Gammon, G. van der Laan, K.W. Goodman, and J.G. Tobin, Phys. Rev. Lett. **81**, 1306 (1998).
30. M.T. Butterfield, J.G. Tobin, N.E. Teslich Jr, R.A. Bliss, M.A. Wall, A.K. McMahan, B.W. Chung, A.J. Schwartz, and A.L. Kutepov, Matl. Res. Soc. Symp. Proc. **893**, 95 (2006).
31. J.J. Yeh and I. Lindau, At. Data Nucl. Data Tables 32, 99 (1985).

Splittings, Satellites and Fine Structure in the Soft X-ray Spectroscopy of the Actinides*

Figure Captions

Figure 1 XAS of the 4d and 5d levels of Pu and U. See text for details. The data are from References 5, 8 and 10.

Figure 2 Experimental setup at LLNL. [19]

Figure 3 Spectroscopic processes are shown here. See text for details.

Figure 4 Schematic of the photoelectron spectroscopy experiment.

Figure 5 XPS of the 4d and 4f levels of Uranium Dioxide. The data are from Ref. 7.

Figure 6 Schematic of the X-ray absorption spectroscopy experiment.

Figure 7 XAS of the Ce 3d and 4d levels, including the corresponding Electron Energy Loss (EELS) spectra and theoretical simulation of the spectra (CALC), performed by G. van der Laan. [21, 22]

Figure 8 LS and jj limiting cases for transitions between the d core levels and near valence f states. This assumes electric dipole selection rules. See text for details.

Figure 9 XAS of Uranium Dioxide. A band gap of 2.1 eV is assumed. [8] CBM is conduction band minimum. The data are from References 8 and 10.

Figure 10 Schematic of the IPES/BIS/RIPES and XES experiments.

Figure 11 Unoccupied Density of States of U. Top panel: Experimental result rom Bremstrahlung Isochromat Spectroscopy (BIS) by Baer and Lang. [17] Bottom panel: Theory with occupied (neg energies) and unoccupied (pos energies) 5f Density of States U calculated by A.L. Kutepov. [4,21,30] See text for details.

Figure 12 BIS of Uranium Dioxide. A band gap of 2.1 eV is assumed. [8] CBM is conduction band minimum. The data are from Reference 10.

Figure 13 RIPES and XES of Uranium Dioxide.

Splittings, Satellites and Fine Structure in the Soft X-ray Spectroscopy of the Actinides*

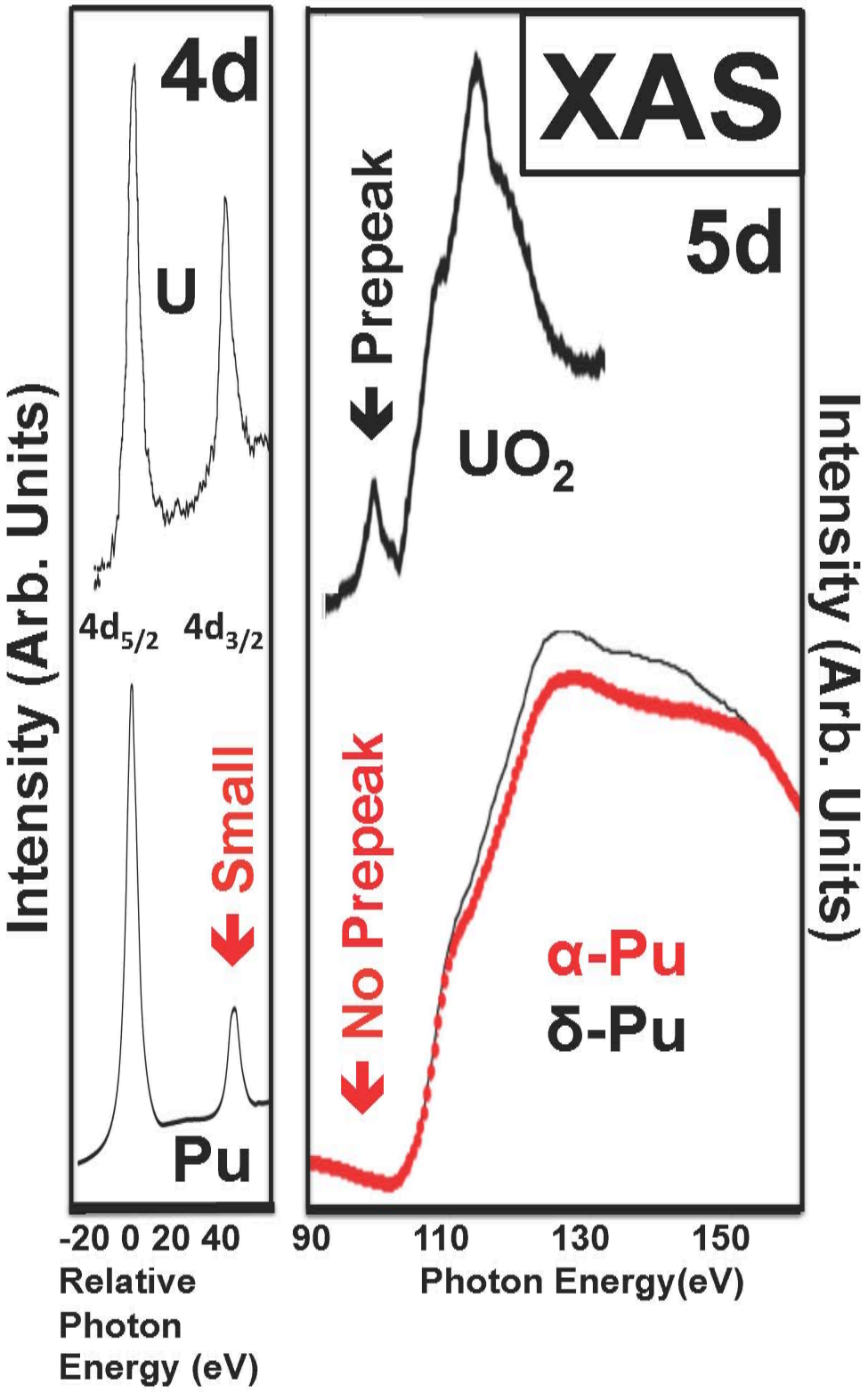

Figure 1

Splittings, Satellites and Fine Structure in the Soft X-ray Spectroscopy of the Actinides*

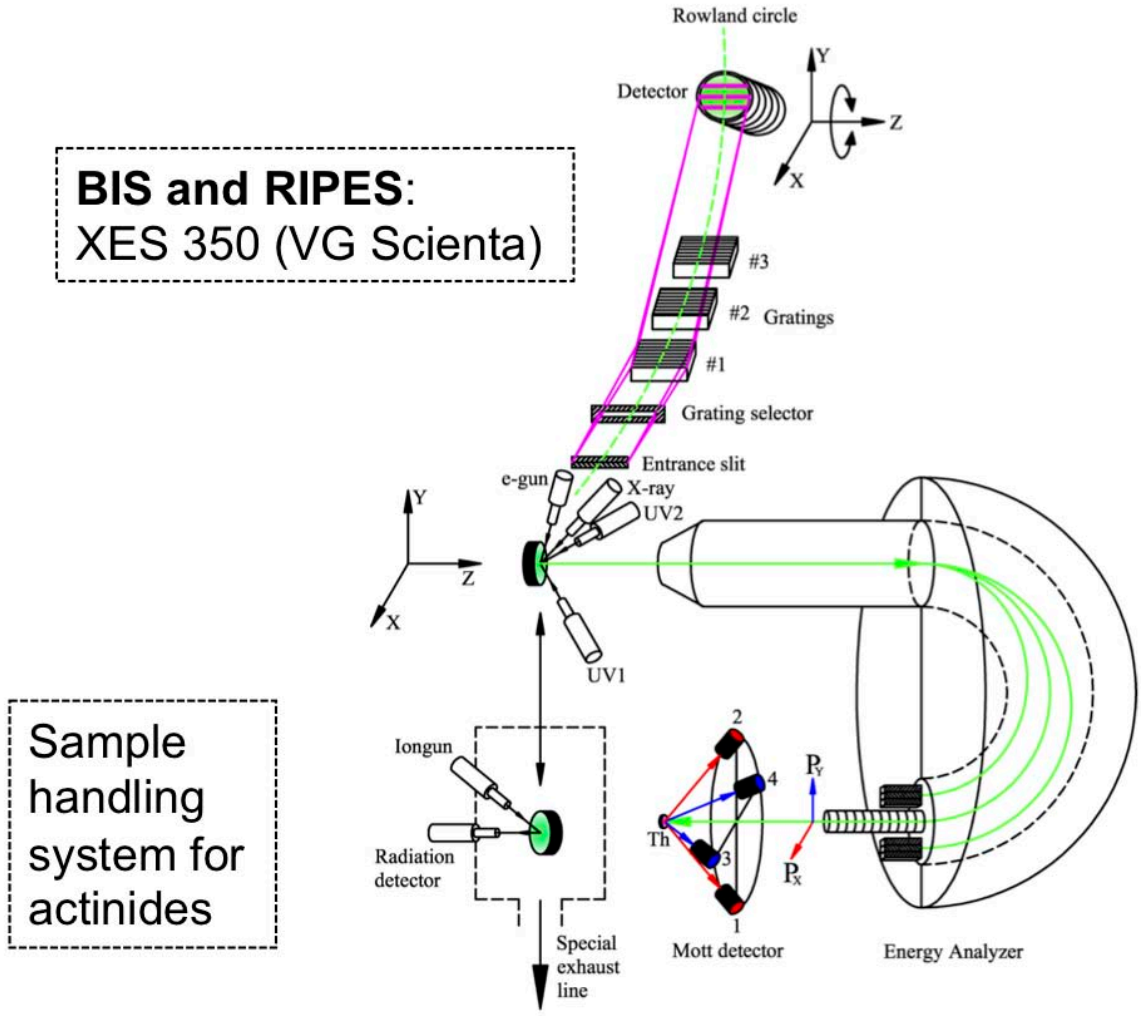

Figure 2

Splittings, Satellites and Fine Structure in the Soft X-ray Spectroscopy of the Actinides*

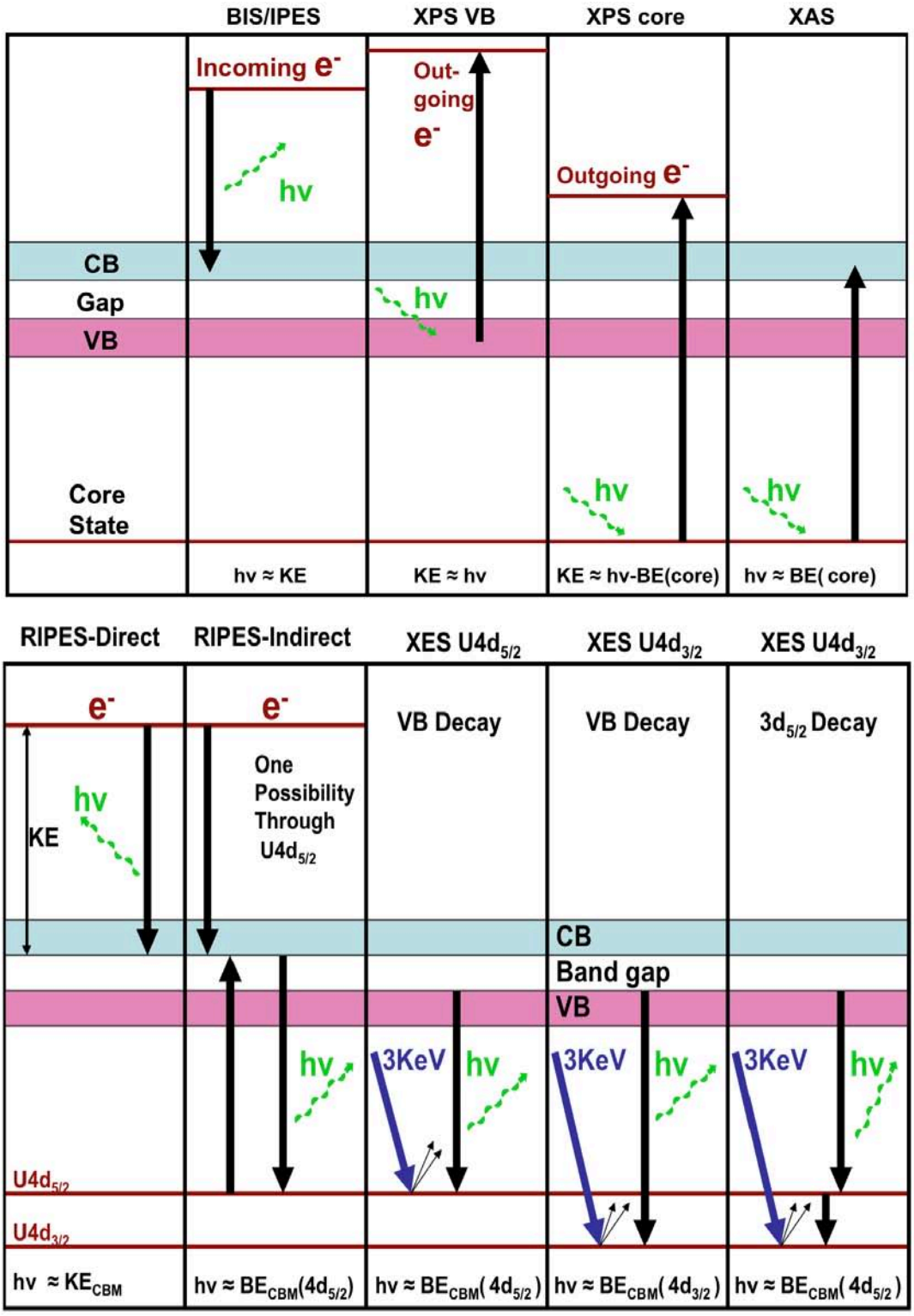

Figure 3

Splittings, Satellites and Fine Structure in the Soft X-ray Spectroscopy of the Actinides*

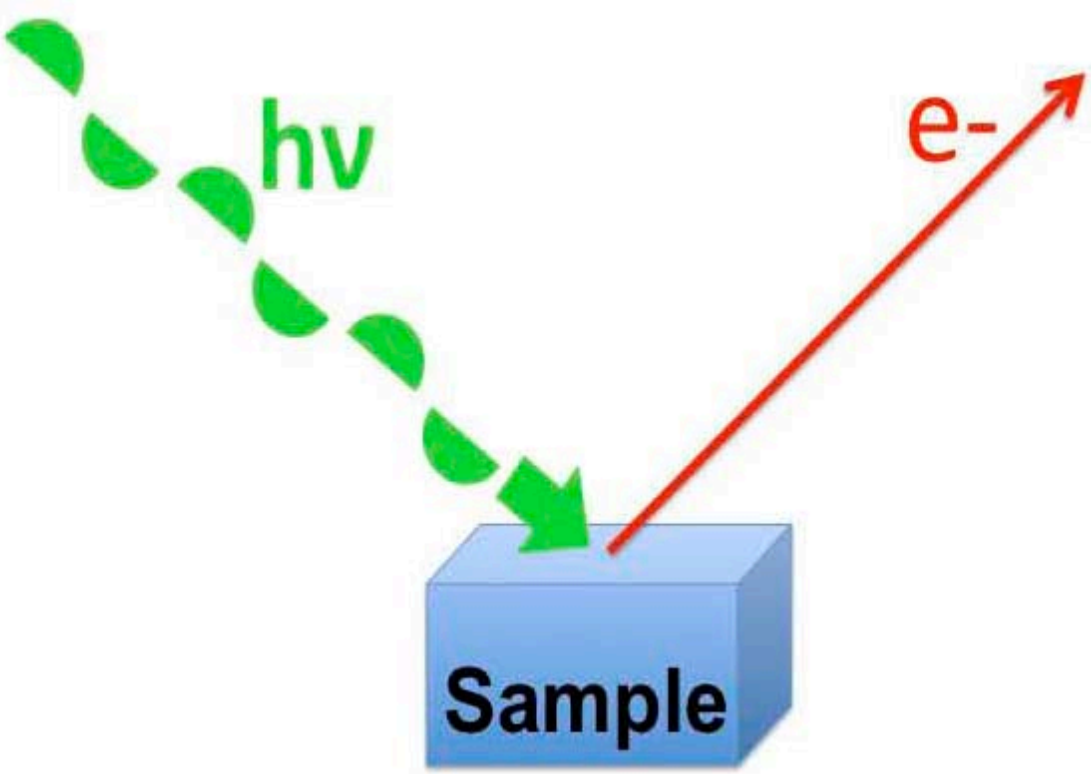

Figure 4

Splittings, Satellites and Fine Structure in the Soft X-ray Spectroscopy of the Actinides*

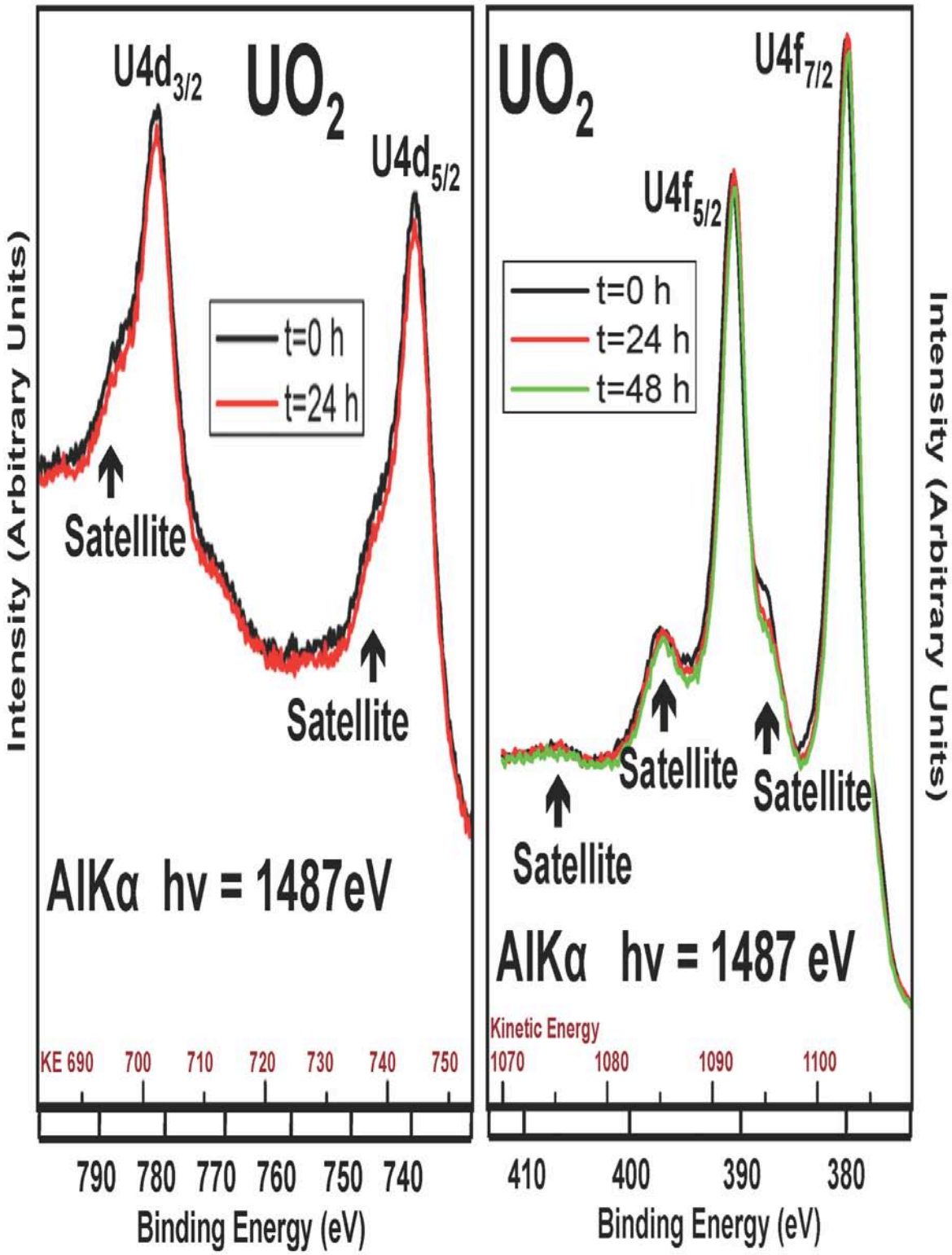

Figure 5

Splittings, Satellites and Fine Structure in the Soft X-ray Spectroscopy of the Actinides*

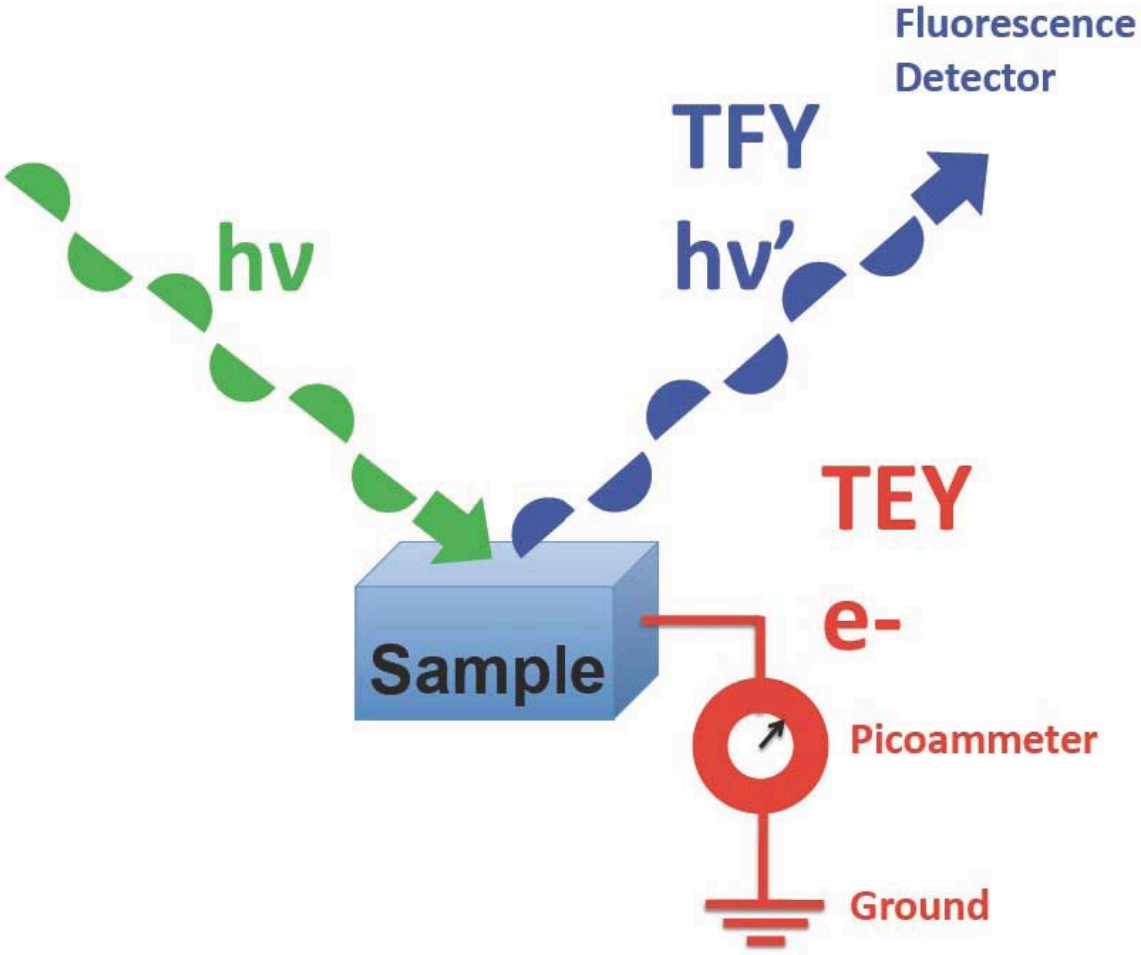

Figure 6

Splittings, Satellites and Fine Structure in the Soft X-ray Spectroscopy of the Actinides*

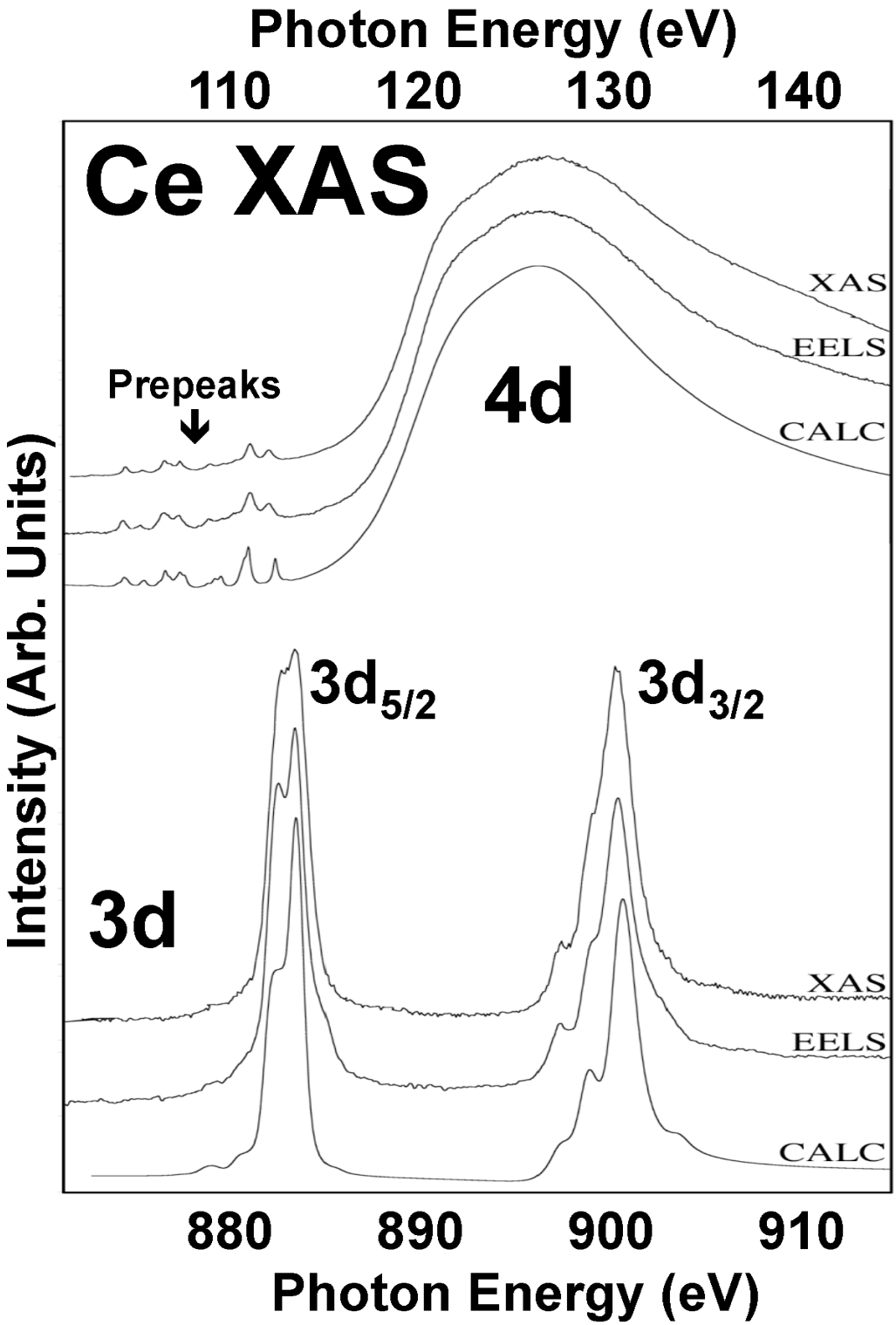

Figure 7

Splittings, Satellites and Fine Structure in the Soft X-ray Spectroscopy of the Actinides*

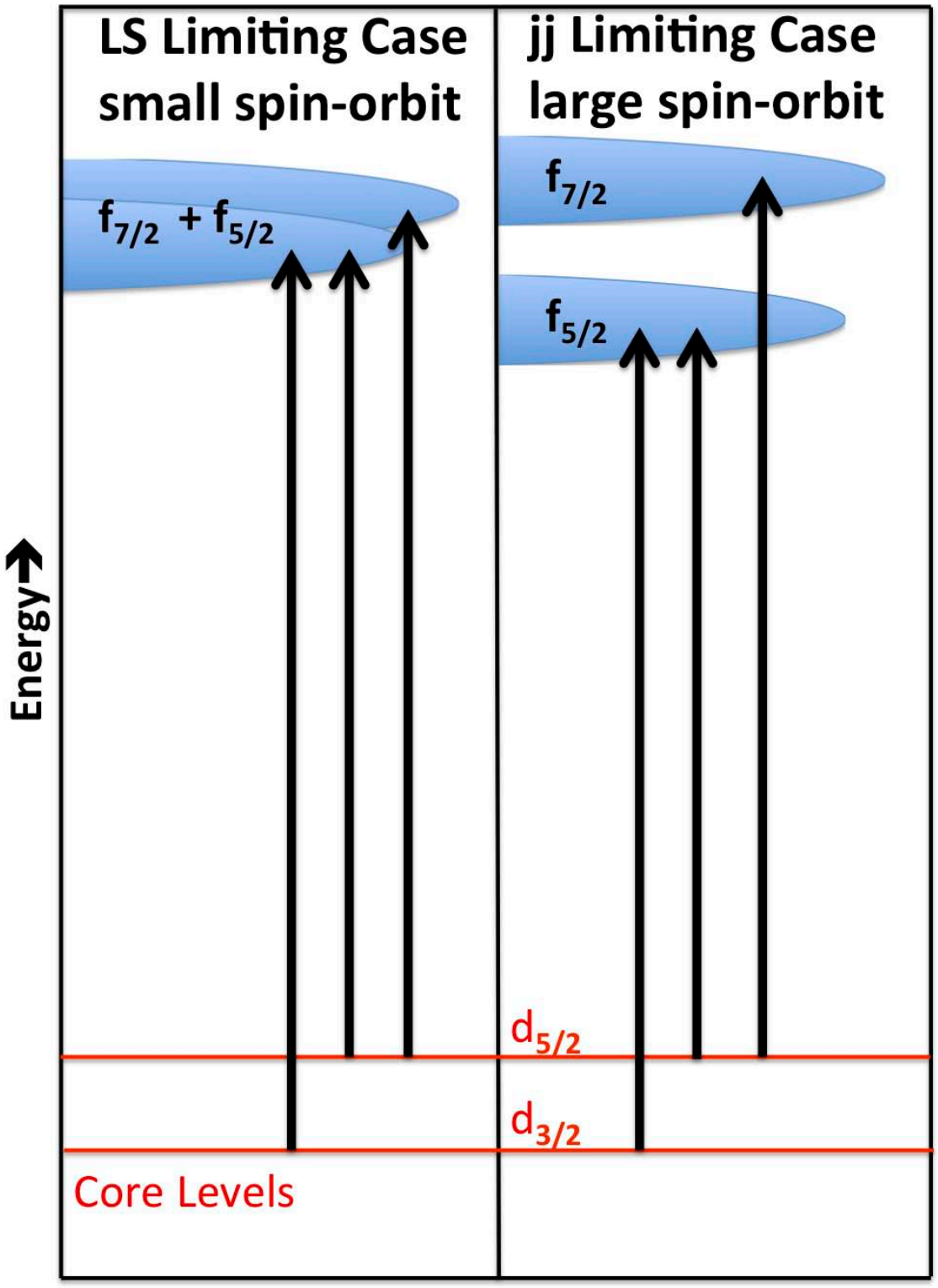

Figure 8

Splittings, Satellites and Fine Structure in the Soft X-ray Spectroscopy of the Actinides*

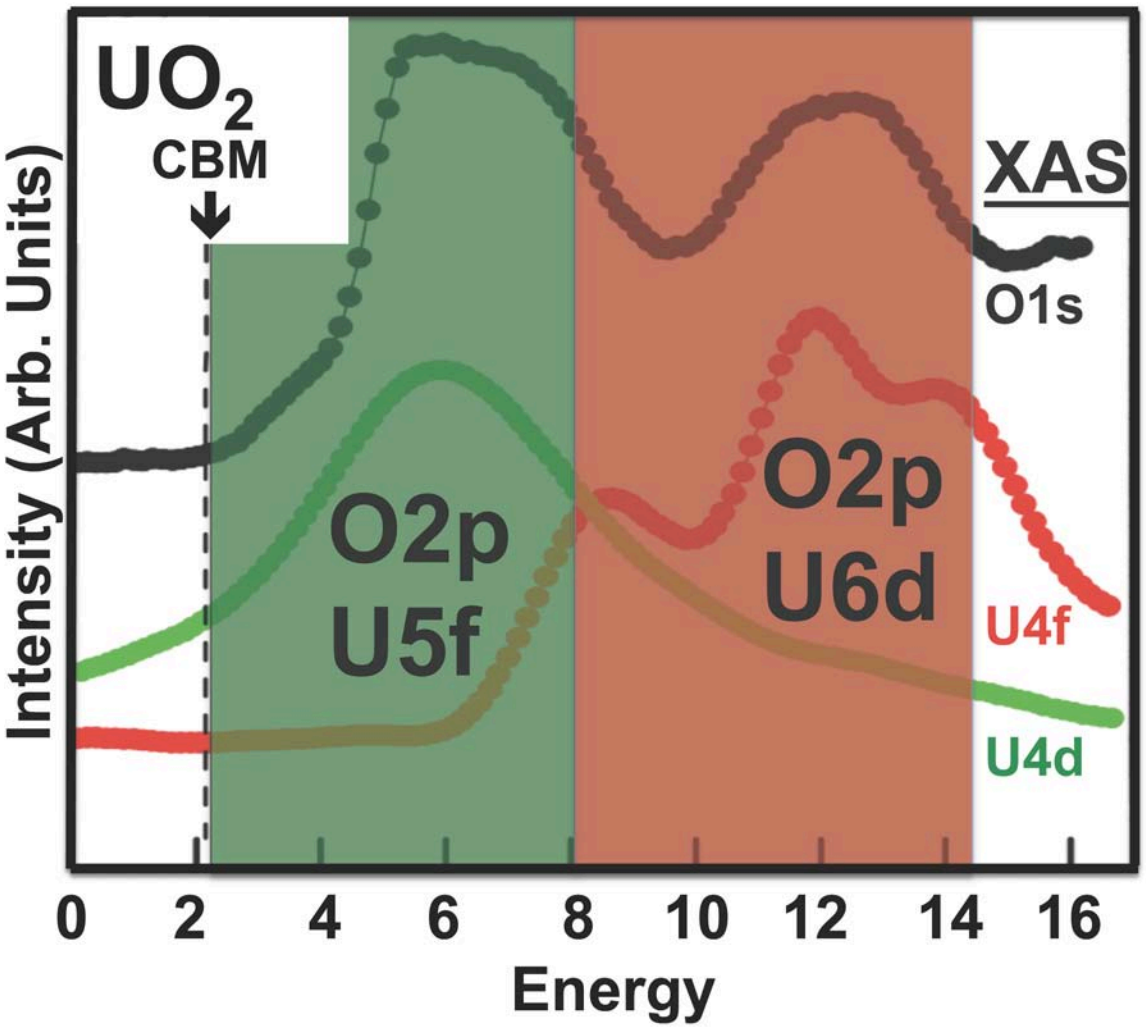

Figure 9

Splittings, Satellites and Fine Structure in the Soft X-ray Spectroscopy of the Actinides*

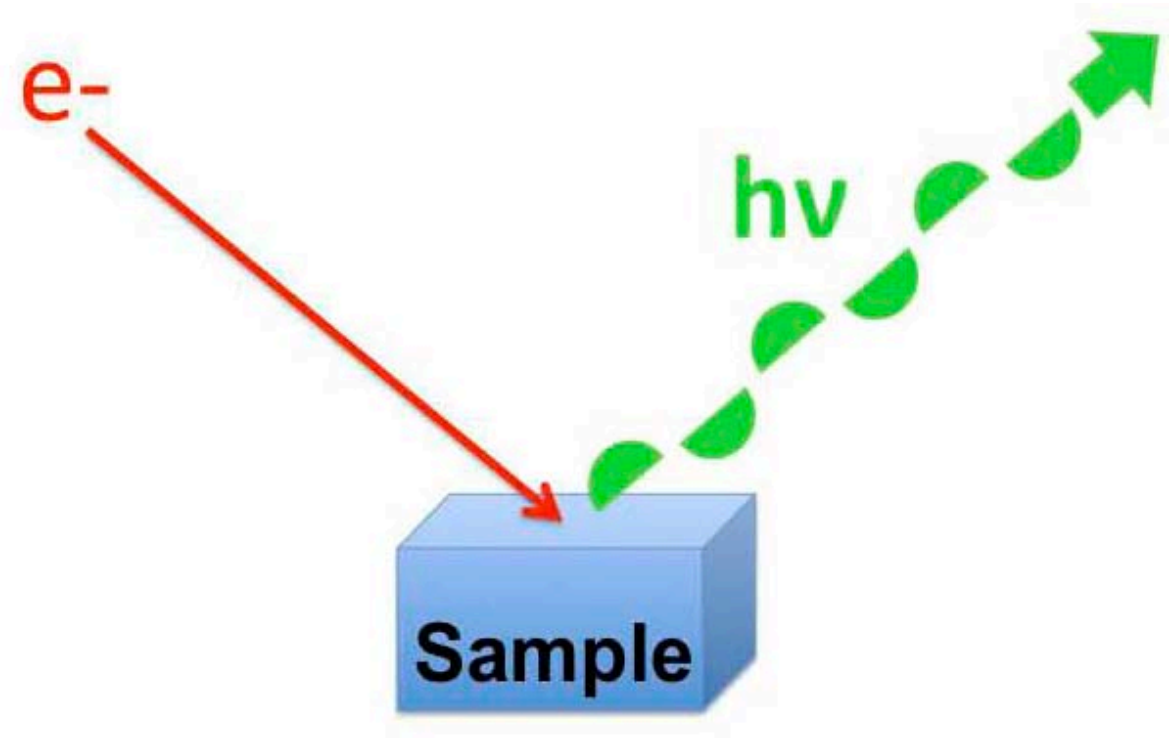

Figure 10

Splittings, Satellites and Fine Structure in the Soft X-ray Spectroscopy of the Actinides*

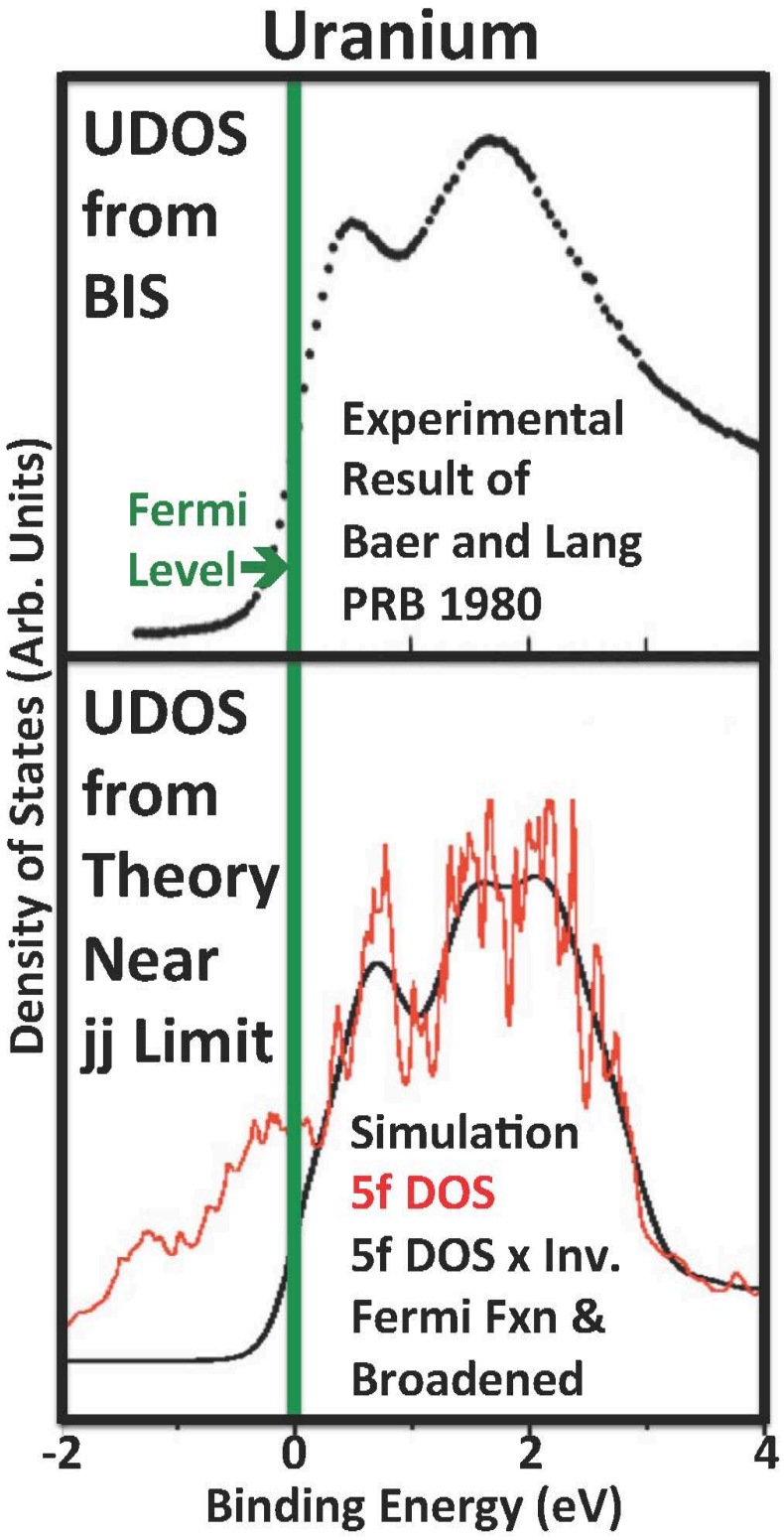

Figure 11

Splittings, Satellites and Fine Structure in the Soft X-ray Spectroscopy of the Actinides*

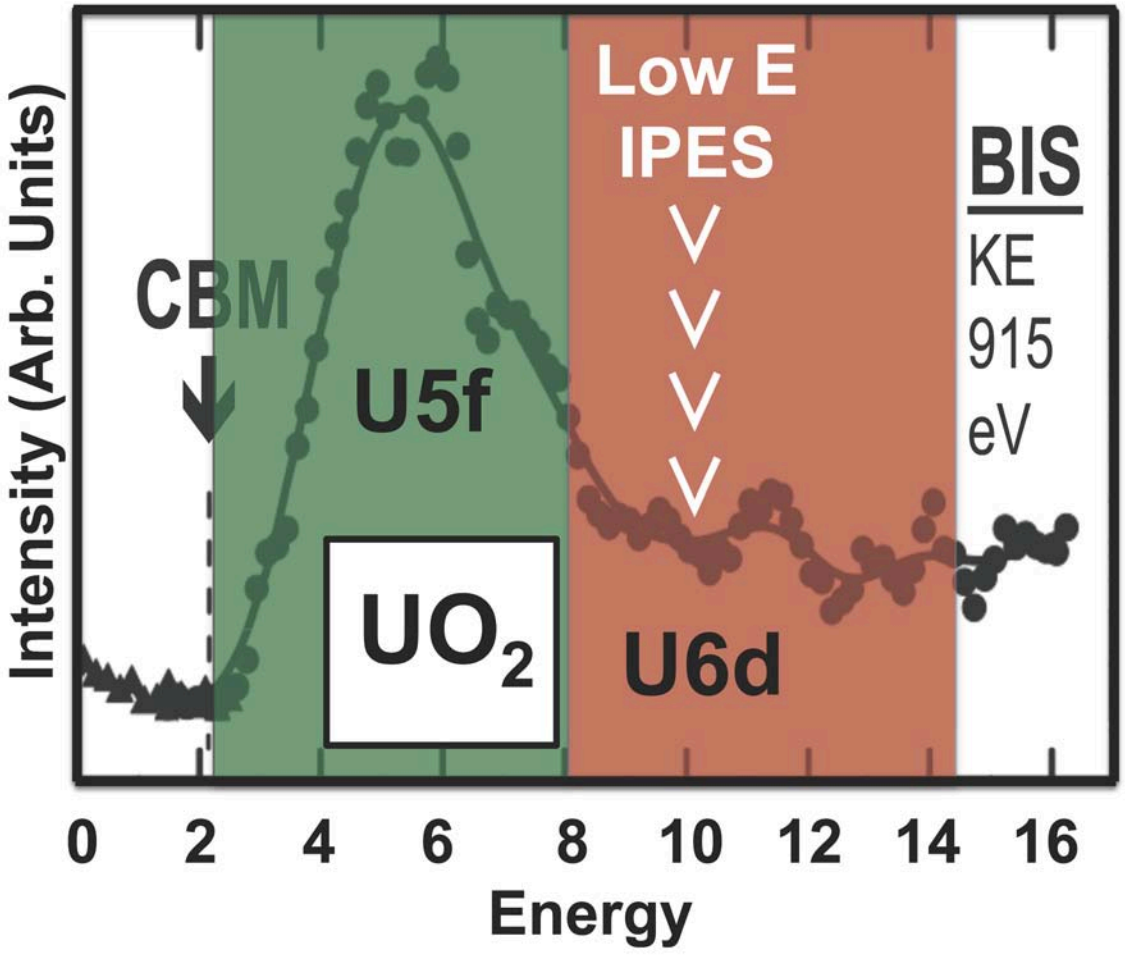

Figure 12

Splittings, Satellites and Fine Structure in the Soft X-ray Spectroscopy of the Actinides*

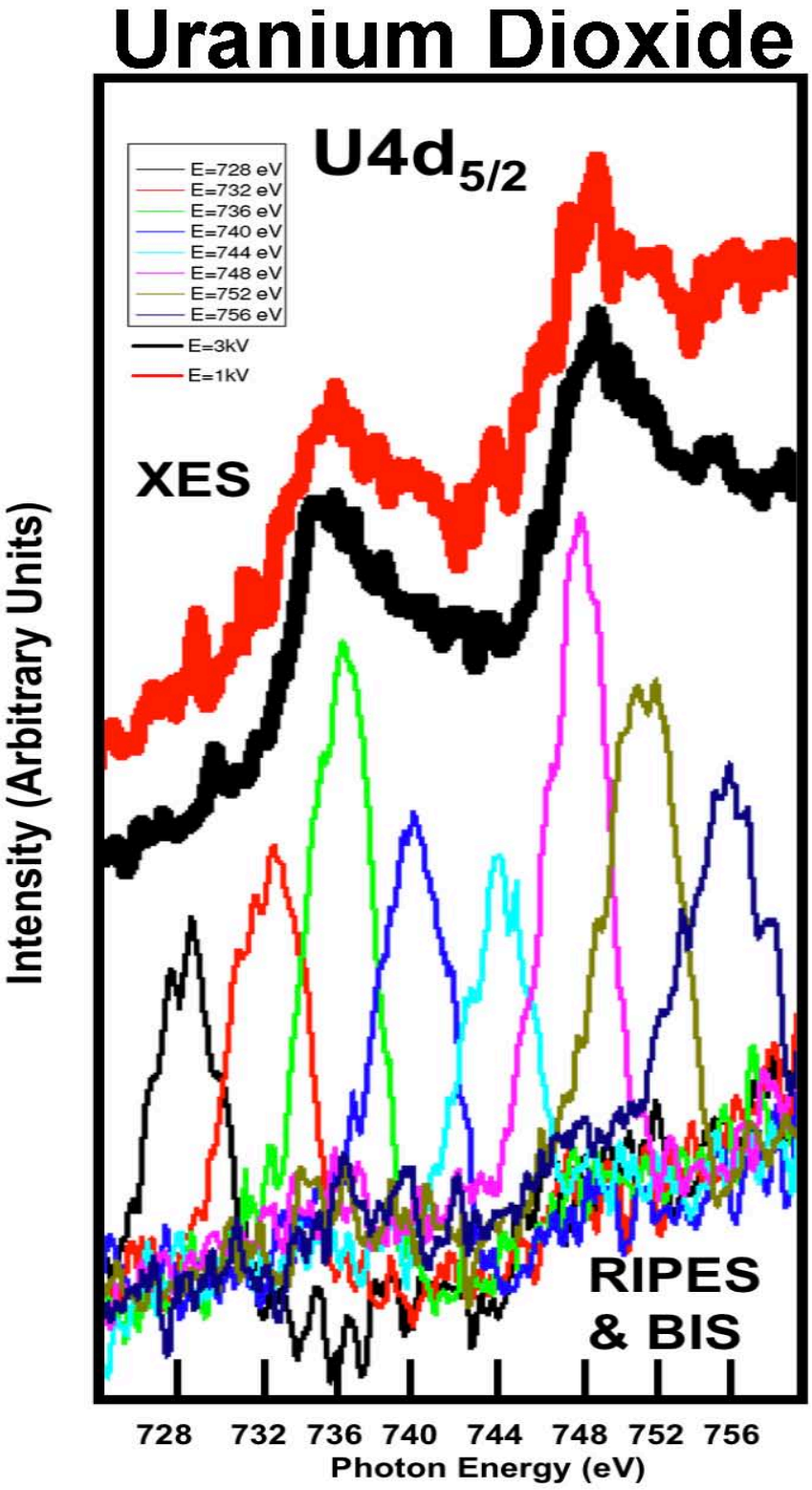

Figure 13